ARTIFICIAL SATELLITES, Vol. 51, No. 4 – 2016
DOI: 10.1515/arsa-2016-0010

HYDROLOGICAL EXCITATIONS OF POLAR MOTION DERIVED FROM DIFFERENT VARIABLES OF $FGOALS - g2$ CLIMATE MODEL

M. Winska
Faculty of Civil Engineering, Warsaw University of Technology, Warsaw, Poland
on sabbatical leave at the Department of Climate and Space Sciences and Engineering, College of Engineering, University of Michigan, Ann Arbor
e-mail: m.winska@il.pw.edu.pl

ABSTRACT. The hydrological contribution to decadal, inter-annual and multi-annual suppress polar motion derived from climate model as well as from GRACE (Gravity Recovery and Climate Experiment) data is discussed here for the period 2002.3-2016.0. The data set used here are Earth Orientation Parameters Combined 04 (EOP C04), Flexible Global Ocean-Atmosphere-Land System Model: Grid-point Version 2 (FGOAL-g2) and Global Land Data Assimilation System (GLDAS) climate models and GRACE CSR RL05 data for polar motion, hydrological and gravimetric excitation, respectively. Several Hydrological Angular Momentum (HAM) functions are calculated here from the selected variables: precipitation, evaporation, runoff, soil moisture, accumulated snow of the FGOALS and GLDAS climate models as well as from the global mass change fields from GRACE data provided by the International Earth Rotation and Reference System Service (IERS) Global Geophysical Fluids Center (GGFC).
The contribution of different HAM excitation functions to achieve the full agreement between geodetic observations and geophysical excitation functions of polar motion is studied here.

Keywords: polar motion, Hydrological Angular Momentum, geodetic residuals

1. INTRODUCTION

The Earth is a dynamical system presenting continually changing global distribution of land fresh water fluids, namely atmosphere, ocean, continually changing global water distribution (ice, water, snow), and its solid part (mobile tectonic plates, earthquakes). These dynamical processes produce torques on the solid Earth causing Earth's rotational to change. These geophysical variations are described as the motion of the rotational axis of the Earth relative to the crust what is called polar motion (X and Y) and changes in the spin rate often expressed in terms of the length-of-day (LOD) variations. These factors that influence on the Earth's rotation variables have been investigated with increasing accuracy for over four decades (Munk and MacDonald, 1960). According to the principle of conservation of angular momentum of the Earth system, rotation of the solid Earth

changes as a result of the transfer of angular momentum between solid Earth and the fluid regions.
There exists many models describing the circulation within the atmosphere, oceans and continental hydrosphere. Due to the fact that these geophysical processes are very complex, these models still suffer from uncertainties in the process description, parameterization and forcing (Güntner, 2008). Consequently, geophysical excitation of Earth rotation, derived from global circulation models, are affected by results from uncertainties, which are difficult to quantify (Gross et al., 2003; Seitz and Schmidt, 2005; Chen and Wilson, 2005; Nastula et al., 2007, 2011; Brzezinski et al., 2009; Dobslaw et al., 2010).

The most significant part of polar motion at seasonal timescales, Atmospheric Angular Momentum (AAM) involves mass (pressure) and motion (wind) terms (Barnes et al., 1983; Chao and Au, 1991; Gross et al., 2003). The pressure term of AAM is the dominant seasonal contributor to wobble, while the wind term of AAM is the most important factor in driving the LOD changes.

The previous studies based on different ocean models, including Ocean Bottom Pressure (OBP) and currents, demonstrate that the oceans also play a major role in the seasonal excitation of the polar motion (Wahr, 1983; Dickey et al., 1993; Ponte et al., 1998; Gross et al., 2003).

The earlier investigations by Gross et al. (2003); Brzezinski et al. (2005) demonstrated that adding the nontidal Oceanic Angular Momentum (OAM) estimate to that of the AAM improves the agreement with the seasonal excitation deduced from the geodetic determinations of Earth orientation. Nevertheless, the sum of AAM and OAM does not entirely explain the observed variations of polar motion, which are determined by geodetic techniques (Ponte et al., 1998; Nastula and Ponte, 1999; Brzezinski et al., 2009). The misfit might be caused by Hydrological Angular Momentum (HAM).

The role of continental hydrology, originating from land water, snow, and ice is however less known than the atmosphere and ocean ones. Nonetheless, Terrestrial Water Storage (TWS) changes also affect polar motion (Chao and O'Connor, 1988), mainly at seasonal timescales.

Previous studies have estimated hydrological excitation of polar motion by using climatological measurements (Van Hylckama, 1970; Hinnov et al., 1987; Chao and O'Connor, 1988) and numerical climate models (Kuehne et al., 1991; Chen et al., 2000). In recent years many studies on the impact of land hydrology on the polar motion excitation give inconsistent results (Chen and Wilson, 2005; Seoane et al., 2011; Nastula et al., 2011; Jin et al., 2012) with very different amplitudes and phases for polar motion excitation at seasonal scales (Nastula et al., 2011; Chen and Wilson, 2005). Indeed, these models do not represent completely hydrological variations (Chen and Wilson, 2005) because Terrestrial Water Storage (TWS) was not adequately measured at the continental scale (Lettenmaier et al., 2006).

To better undestand the changes in hydrological part excitation of polar motion, and to indicate global and regional influence of selected variables on polar motion excitation, the fifth version of the Coupled Model Inter-comparison Project-Phase 5 (CMIP5) experiment design has been chosen. The HAM time series used in these studies were estimated from Flexible Global Ocean-Atmosphere-Land System Model: Grid-point Version 2 (FGOALS-g2). In this study the water storage is the sum of soil moisture and snow water equivalent and precipitation, evaporation and total runoff not counting changes in groundwater below the depth defined by the model.

Since 2002 the Gravity Recovery and Climate Experiment (GRACE) satellite mission and since 1980 to lesser extent the Laser Geodynamics Satellite (LAGEOS) mission has delivered precise time series of gravimetric variations and has allowed to determine the mass-gravimetric polar motion excitation function. Indeed, the coefficients of the second degree and of the first order of the Earth gravity field are proportional to variations of the equatorial component χ_1, χ_2 of the series of the gravimetric excitation function of polar motion. This gravimetric function can be considered as the mass term of polar motion excitation. The gravimetric excitation functions estimates from Equivalent Water Thickness (EWT) GRACE are subject to de-striping, gridded mapping and filter smoothing methods as well as to aliasing errors (Jin et al., 2010). Several centers, such as the GeoForschungsZentrum (GFZ), the Center for Space Research (CSR), and the Jet Propulsion Laboratory (JPL) have computed the time series of second degree geopotential and of the water storage (Brzezinski et al., 2009; Chen and Wilson, 2005; Seoane et al., 2009). In this study we used the GRACE data of RL05 series as computed by CSR.

In papers by (Jin et al., 2010, 2012; Nastula et al., 2011), the global hydrological and gravimetric excitation functions of polar motion were compared with the residual series $GAO{=}GAM{-}AAM{-}OAM$ as computed by removing atmospheric (AAM) and oceanic (OAM) contributions from the Geodetic Angular Momentum GAM series (Nastula et al., 2011). In this study the GAM were derived from the pole coordinates time series C04 provided by International Earth Rotation and Reference System Service (IERS) (Bizouard and Gambis, 2009). The atmospheric excitation function AAM is derived from the time series of NCEP/NCAR reanalysis data (Salstein et al., 1993). The OAM, including bottom pressure and currents term, were computed on the basis of the ECCO-JPL ocean model (Gross et al., 2003).

Here we use different output from CMIP5 - FGOALS-g2 model at decadal, inter-annual and muli-annual timescales. In parallel we use the GRACE mass component of polar motion excitation as well as global terrestrial water storage from global land assimilation system (GLDAS), considered in earlier studies (e.g. Chen and Wilson (2005); Nastula et al. (2011); Meyrath et al. (2013)).

Our investigations aims at characterizing the separate hydrological processes influence of land surface (precipitation, evaporation, total runoff, soil moisture, snow) on polar motion excitation functions. We are looking for climate models which can account for geodetic residuals GAO by hydrological excitation functions of polar motion.

2. METHODS AND DATA DESCRIPTION

Hydrological excitations of polar motion are computed according to (Eubanks, 1993):

$$\begin{bmatrix} \chi_1 \\ \chi_2 \end{bmatrix} = -\frac{1.098R_e^2}{C-A} \iint \Delta q(\phi, \lambda, t) \pm sin(\phi)cos(\phi) \begin{bmatrix} cos(\lambda) \\ sin(\lambda) \end{bmatrix} dS, \tag{1}$$

where $\Delta q(\phi,\ \lambda,\ \mathrm{t})$ represent the changes in water storage in unit area (in kg/m^2), R_e is the Earth's mean radius, dS is the surface element area, and C and A are the Earth's principal moment of inertia. The factor 1.098 accounts for the combined effects of the yielding of the solid Earth to the surface load, core-mantle decoupling and rotational deformations (Eubanks, 1993).

The terrestrial water storage (TWS) change $\Delta q(\phi, \lambda, t)$ is computed on a monthly basis, firstly considering the model:

$$\Delta TWS1 = (TWS1)_{n+1} - (TWS1)_n = P_n - E_n - R_n, \tag{2}$$

where P is precipitation, E is a sum of water evaporation from soil and the canopy evaporation, R is a total surface runoff leaving the land portion of the grid cell, subscripts n and $n+1$ indicate present and next month, respectively.

TWS comprises all the components of the terrestrial water: biomass, surface water, ice, snow, soil moisture, and groundwater.

Secondly, monthly TWS changes are calculated according to

$$\Delta TWS2 = (TWS2)_{n+1} - (TWS2)_n = (SM_{n+1} + SNW_{n+1}) - (SM_n + SNW_n), \tag{3}$$

where SM is soil moisture content, SNW is an accumulated snow content.

These data were taken directly from FGOALS-g2 climate model at 1 month sampling rate, $2.8^0 \times 2.8^0$ latitude and longitude grid.

The TWS1 changes are computed using output fields of monthly average precipitation (P) rates in all phases, monthly average surface latent heat flux (HFLS), which is converted to evaporation by dividing HFLS by the latent heat of vaporization, and monthly average total runoff (MRRO). We estimated TWS2 changes using the variable 'mrso' that is the monthly averaged soil moisture in all phases summed over all model soil layers and averaged over the land portion of the grid cell, the variable 'snw' that is the sum over all snow layers and grid area averaged.

Changes of Terrestrial Water Storage $\Delta q(\phi, \lambda, t)$ based on the gravity data are computed from the spherical harmonic coefficients of the Earth's gravity field (Wahr et al., 1998). Global mass change fields are obtained from GRACE CSR RL05 data series given at monthly sampling rate, $1.0^0 \times 1.0^0$ latitude and longitude grid and 500 km decorrelation Gaussian smoothing.

Finally, we computed the hydrological excitation functions associated with the GLDAS NOAH climate model (Rodell et al., 2013).

2.1. MODELED HYDROLOGICAL EXCITATION OF POLAR MOTION

The Flexible Global Ocean-Atmosphere-Land System Model, Grid point Version 2 ($FGOALS-g2$), used in this study, is a climate model from the fifth phase of the Coupled Model Intercomparison Project ($CMIP5$) which is composed of separate component models of the atmosphere, ocean, sea ice, and land surface (Li et al., 2013). FGOALS-g2 is one of

the newest version of FGOALS; it has been developed by a community of scientists and graduate students from the Laboratory of Numerical Modeling for Atmospheric Sciences and Geophysical Fluid Dynamics (LASG), the Institute of Atmospheric Physics (IAP) of the Chinese Academy of Sciences, Center for Earth System Science (CESS)/Tsinghua University, and the First Institute of Oceanography (FIO)/State Oceanic Administration. The land-surface component is the Community Land Model, version 3 (CLM3.0) and has 10 soil layers in the vertical direction (Oleson et al., 2004).
Several Hydrological Angular Momentum (HAM) functions are calculated here from the selected variables of the FGOALS-g2 climate model. FGOALS includes soil moisture and snow water, but omits polar ice sheets in Antarctica.

Global terrestrial water storage contributions to polar motion excitations are also estimated from GLDAS model (Rodell et al., 2013). GLDAS includes soil moisture and snow water but omits mountain glaciers and polar ice sheets in Greenland and Antarctica. It is forced by atmospheric input of NOAA/GLDAS models of Precipitation (CMAP) fields of the NOAA and shortwave and long wave radiation fields derived by the Air Force Weather Agency's AGRicultural METeorological modeling system (AGRMET). The simulations are initialized on 1 January 1979 using soil moisture and other state fields from a GLDAS model for that day of the year.

2.2. GRAVIMETRIC EXCITATION OF POLAR MOTION

The GRACE data are provided by different centers in the form of normalized spherical harmonic coefficients. In this study, the GRACE CSR RL05 version of the gravity field solution was used. The data are available in terms of equivalent water height changes given by IERS Global Geophysical Fluid Center (GGFC) Special Bureau for the Hydrology. The calculated gravimetric excitation functions are tide free, the non-tidal atmospheric and oceanic effects have been removed from the gravimetric data (Chen et al., 2004). Then gravimetric -based excitation shows variations not only from hydrological processes, but also from post-glacial rebound, earthquakes and resulting other smaller but unknown Earth's geophysical phenomena.
The gravimetric polar motion excitation function is directly related to the (2,1) Stokes coefficients of the gravity field and to the inertia tensor of the Earth in the terrestrial reference frame.
In order to unify considerations as well as to focus on inter-annual, seasonal, and multi-annual periodicities, all the time series were smoothed by the Gaussian method with a step of thirty days.

3. RESULTS AND DISCUSSIONS

3.1. OVERALL COMPARISON

After removing mass and motion contributions of atmosphere and ocean from the observed polar motion, the geodetic residuals GAO of χ_1 and χ_2 components for 2002.3-2015.9 are compared with global hydrological excitation functions computed from GLDAS climate model and from FGOALS-g2 variables, and with gravimetric excitation functions computed from GRACE data. Monthly mass-land excitations are shown in the Fig. 1. Geodetic residuals GAO (black curve) and gravimetric excitation functions (red curve), for both χ_1 and χ_2 components are composed of infra-seasonal, inter-annual (1.5−2 years),

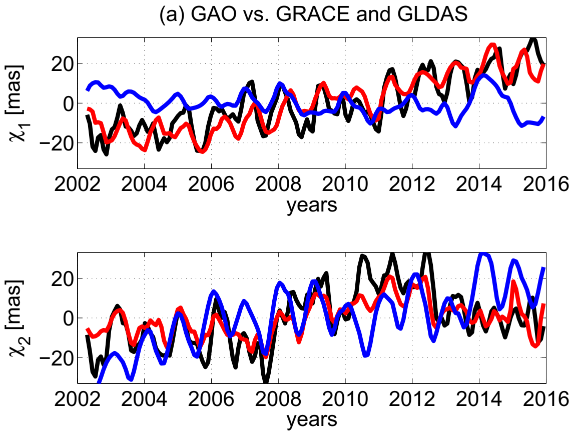

(a) GAO (black) vs. GRACE (red), GLDAS (blue)

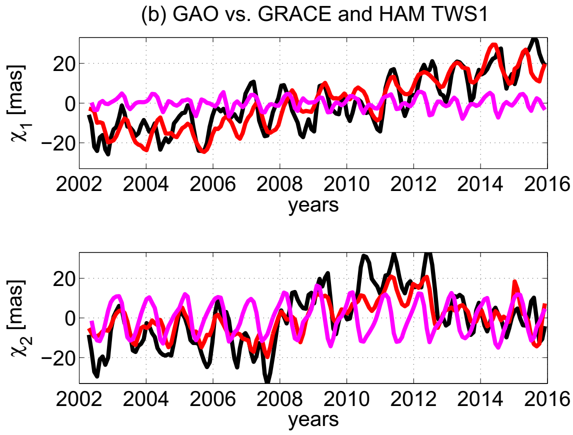

(b) GAO (black) vs. GRACE (red), TWS1 (magenta)

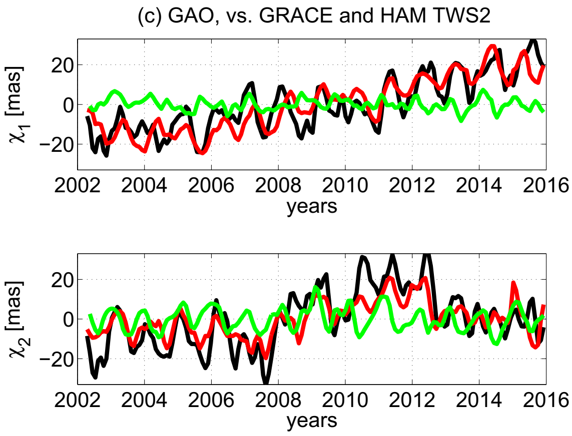

(c) GAO (black) vs. GRACE (red), TWS2 (green)

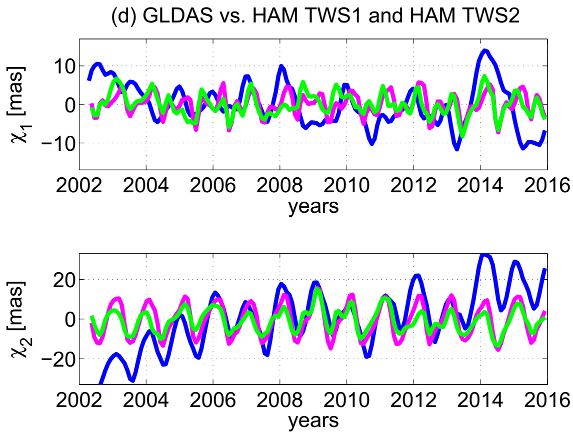

(d) TWS1 (magenta) vs. TWS2 (green), vs. GLDAS (blue)

Figure 1. Monthly land mass-term excitation functions derived from observed polar motion excitations χ_1 and χ_2 (black curves) by removing AAM and OAM, hydrological contributions observed by GRACE (red curves), hydrological contributions determined from land-based climate model GLDAS (blue curves), and hydrological excitation functions determined from different output of FGOALS-g2 climate model of the CMIP5 project: (a) GAO vs. GRACE and GLDAS , (b) GAO vs. GRACE and TWS1 determined from Equation 2 (magenta curves) and (c) GAO vs. GRACE and TWS2 determined from Equation 3 (green curves); (d) comparison of different HAM excitations: TWS1, TWS2, GLDAS.

multi−annual and multi−decadal (>20 years) terms.
Those global hydrological excitation functions, which are determined from different variables of FGOALS-g2 climate model, have a smaller oscillations, especially in the χ_1 component (Fig. 1b, 1c, 1d).
Figure 1d shows estimates of χ_1 and χ_2 variations of HAM excitations computed from different variables of FGOALS-g2 climate model and from GLDAS model. The HAM estimates of TWS1 and TWS2 are similar to one another. Wherein the time series of χ_2 components fit better the geodetic residuals GAO, gravimetric excitation functions, and GLDAS HAM functions, both in their amplitudes and phases.

3.2. LINEAR TREND

Hydrological excitation, their gravimetric and geodetic counterpart as well, present trend, especially considerable for χ_2 component and GLDAS model. These trends result from the solid Earth Post Glacial Rebound effects, and from climate changes (Chen et al., 2013).
Over 14 years of data, trends are assimilated to linear terms, which are fitted and reported in Tab.1. In this respect only TWS1 CMIP5, GRACE and geodetic residuals GAO rates in χ_2 component are comparable (Fig. 1a, 1b, Table 1).

Table 1: Land-based hydrology mass-term polar motion excitation rates for χ_1 and χ_2 from polar motion observations (GAO), GRACE data estimates for mass changing over the lands, GLDAS and from outputs of the FGOAL-g2 climate model.

Land mass excitations	χ_1 Rate (mas/yr)	χ_2 Rate (mas/yr)
GAO	2.80 ± 0.06	1.65 ± 0.08
GRACE	3.10 ± 0.14	1.03 ± 0.16
GLDAS	-0.58 ± 0.10	3.00 ± 0.20
TWS1 CMIP5	0.03 ± 0.07	0.95 ± 0.16
TWS2 CMIP5	0.02 ± 0.07	0.22 ± 0.12

3.3. INTER-ANNUAL AND SEASONAL VARIATIONS IN POLAR MOTION EXCITATIONS

Figure 2 shows inter-annual period of χ_1 and χ_2 time series for geodetic residuals GAO, gravimetric excitations from GRACE, GLDAS hydrological excitations and the different HAM excitations TWS1, and TWS2. Here, linear trends are removed and Gaussian smoothing with the FWHM=60 days is applied. The 182.6 and 121.8 day terms are removed from time series using least square methods. There is good agreement among inter-annual variations, especially in χ_2, and between geodetic residuals GAO and GRACE excitations. Considering global HAM variations from FGOALS-g2 climate model, the best agreement occurs between TWS1 and GLDAS excitation functions in the case of χ_2 component (see Figure 2d). Meanwhile for χ_1 components again FGOALS-g2 HAM excitations are much smaller than the other contributions. According to Figure 2d, inter-annual FGOALS-g2 HAM excitations, χ_1 and χ_2 components agree pretty well, especially for the χ_2 component, but the TWS2 HAM excitation has a smaller amplitude. It indicates that soil moisture and accumulated snow variables are underestimated.

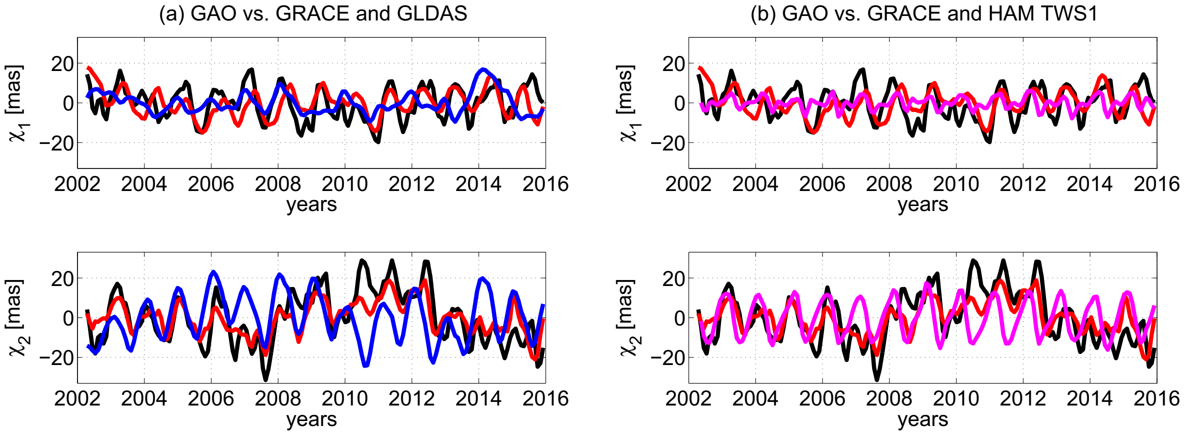

(a) GAO (black) vs. GRACE (red), GLDAS (blue)

(b) GAO (black) vs. GRACE (red), TWS1 (magenta)

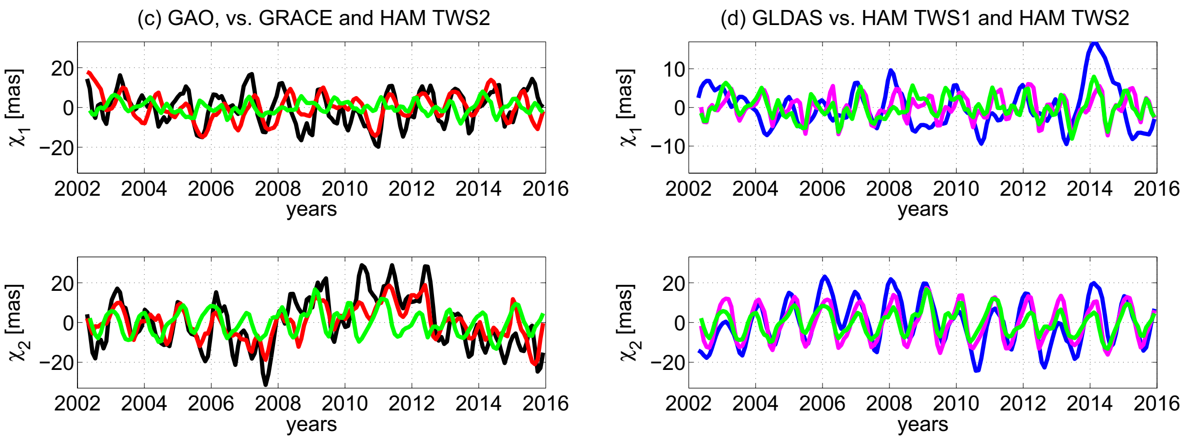

(c) GAO (black) vs. GRACE (red), TWS2 (green)

(d) TWS1 (magenta) vs. TWS2 (green), vs. GLDAS (blue)

Figure 2. Monthly inter-annual land mass-term excitations functions derived from observed polar motion excitations GAO (black curves), by removing AAM and OAM, climate contributions observed by GRACE (red curves), hydrological contributions determined from land-based climate model GLDAS (blue curves), and hydrological excitation functions determined from different output of FGOALS-g2 climate model of the CMIP5 project: (a) GAO vs. GRACE and GLDAS, (b) GAO vs. GRACE and TWS1 (magenta curves), (c) GAO vs. GRACE and TWS2 (green curves), (d) comparison of different HAM excitations: TWS1, TWS2, GLDAS.

Table 2: Amplitudes and phases of prograde and retrograde both annual and semiannual oscillations of geodetic residuals GAO, different HAM excitation functions and its components and of GRACE gravitational excitation functions of polar motion. Phase ϕ is defined here by the annual and semiannual term as $\sin(2\pi(t-t_0)+\phi)$, where t_0 is a reference epoch for January 1 2002.

Model	Annual amplitudes		Annual phases	
	Prograde [*mas*]	*Retrograde* [*mas*]	*Prograde* [*degree*]	*Retrograde* [*degree*]
$G-A-O$	4.4±0.6	4.7±0.6	-47.5 ± 7.3	135.3 ± 6.9
$GRACE$	2.1±0.9	5.8±0.9	-58.0 ± 24.0	132.7 ± 8.8
$GLDAS$	6.6±0.9	5.5±0.8	51.1 ± 7.5	110.9 ± 8.3
$TWS1$	6.6±0.5	5.7±0.5	-77.5 ± 4.6	101.1 ± 5.2
$TWS2$	3.5±0.6	3.7±0.5	-61.5 ± 10.2	94.5 ± 7.6
Model	**Semi-annual amplitudes**		**Semi-annual phases**	
	Prograde [*mas*]	*Retrograde* [*mas*]	*Prograde* [*degree*]	*Retrograde* [*degree*]
$G-A-O$	2.4±0.5	2.1±0.4	116.3 ± 12.7	91.3 ± 11.3
$GRACE$	1.7±0.9	0.7±0.9	123.9 ± 28.8	45.2 ± 70.9
$GLDAS$	0.4±0.9	2.1±0.6	126.9 ± 112.0	1.5 ± 17.3
$TWS1$	3.2±0.9	2.4±0.9	-146.2 ± 16.3	46.8 ± 22.2
$TWS2$	1.6±0.7	2.0±0.7	-120.5 ± 26.7	18.3 ± 20.0

Amplitudes and phases of prograde and retrograde annual and semi-annual variations are determined from each of the complex-valued $\chi_1 + i\chi_2$ time series using least squares method, with results listed in Table 2. Here, TWS1 HAM and GLDAS HAM excitations agree well in both prograde and retrograde amplitudes, as well as in retrograde annual phase. The TWS2 HAM has smaller annual amplitudes than geodetic residuals GAO both in prograde and retrograde oscillations. In the case of semi-annual oscillations, TWS1 HAM prograde and retrograde oscillations are the strongest one and comparable with geodetic residuals GAO, but their phase differences with geodetic residuals GAO are large.

For visual comparison of seasonal amplitudes, we show in Fig. 3 complex Fourier spectra of the geodetic residuals GAO and of the HAM excitation functions determined from GLDAS model, different realization of FGOALS-g2 climate model as well as from GRACE RL05 data. These spectra are computed using Fourier Transform Band Pass Filter (FTBF; Kosek (1995)) in the broad band with 50 and 450 day cutoff. The spectra of all considered functions show annual, semiannual and 120 - day periods oscillations, both in the prograde and retrograde band.

In spectra of HAM excitation functions, GLDAS, TWS1, TWS2, geodetic residuals GAO and GRACE gravimetric excitations, the most energetic oscillation is the annual signal. The prograde annual oscillation of the geodetic residuals GAO has a greater amplitude than that of the considered HAM functions, but in the case of retrograde annual oscillations the GRACE, TWS1 HAM and GLDAS HAM excitations are more powerful than geodetic residuals GAO. The semiannual HAM contributions are smaller than geodetic residuals, excepting TWS1.

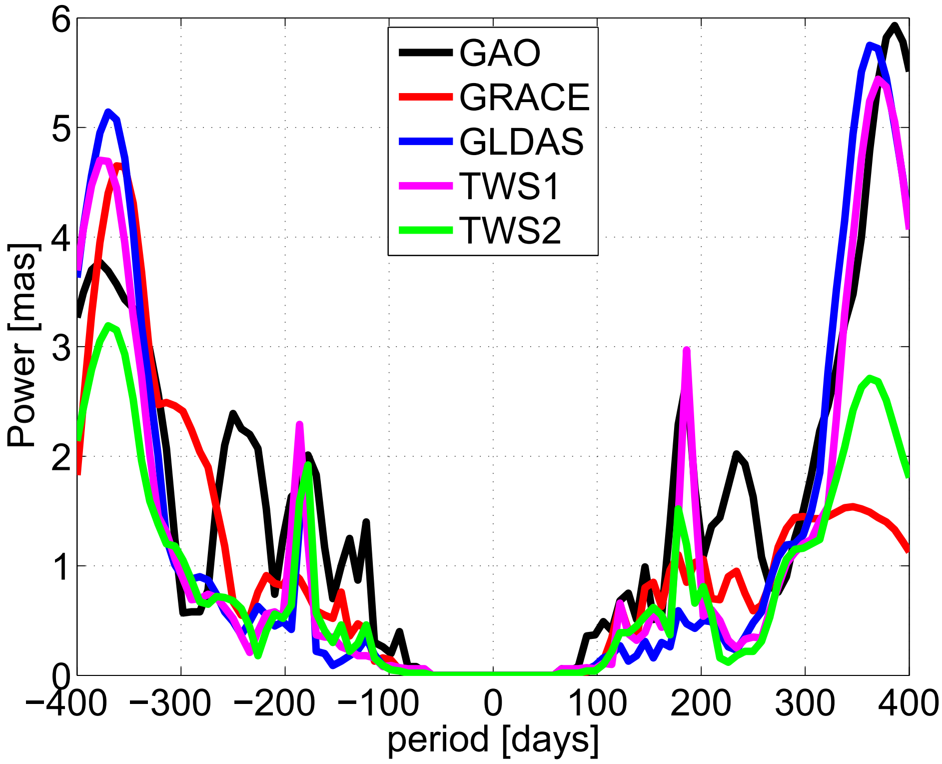

Figure 3. Fourier Transform Band Pass Filter (FTBPF) amplitude spectra of the geodetic residuals G-A-O as well as of the different complex hydrological excitation functions computed from GLDAS model and different variables of FGOALS-g2 climate model (precipitation, evaporation, total runoff, and soil moisture, surface snow amount) and from GRACE data.

3.4. MULTI-ANNUAL VARIATIONS IN POLAR MOTION EXCITATIONS

The multi-annual excitation functions of polar motion were isolated after removing the 365.25 and 182.6 day oscillations from time series and are shown in the Fig.4. None of the HAM excitation functions obtained from FGOALS-g2 climate model agree with geodetic residuals, or gravimetric excitation functions. However, TWS2 χ_2 excitation almost reach the GRACE excitation amplitude (Fig. 4c). GLDAS HAM multi-annual excitations do not agree with geodetic residuals and GRACE data. In the Figure 4d, remarkable good agreement between TWS1 HAM and TWS2 HAM is shown. While a nonseasonal oscillations of GLDAS HAM excitations are bigger.

Looking for correlations between nonseasonal geodetic residuals and other geophysical excitation functions of polar motion, the wavelet-based semblance analysis were used here (Cooper and Cowan, 2008). These semblance filtering compares two datasets based on correlations between their phase angles, as a function of frequency. The results, showing semblances between geodetic residuals GAO and other HAM and gravimetric excitation functions, in both χ_1 and χ_2 components, are shown in the Figure 5. Bright red color corresponds to a semblance of $+1$, green to a semblance of zero, and dark blue to a semblance of -1. Semblance between geodetic residuals GAO and (a) gravimetric excitation functions computed from GRACE data, (b) hydrological excitation functions computed from GLDAS climate model, (c) hydrological excitation functions computed from TWS1

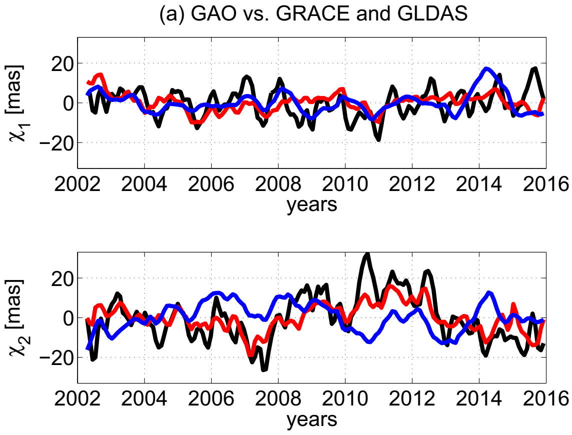

(a) GAO (black) vs. GRACE (red), GLDAS (blue)

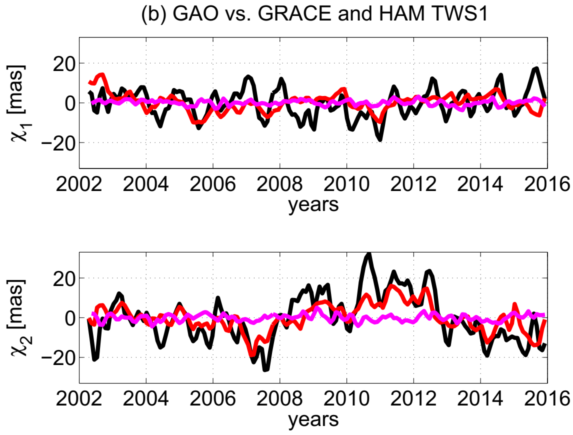

(b) GAO (black) vs. GRACE (red), TWS1 (magenta)

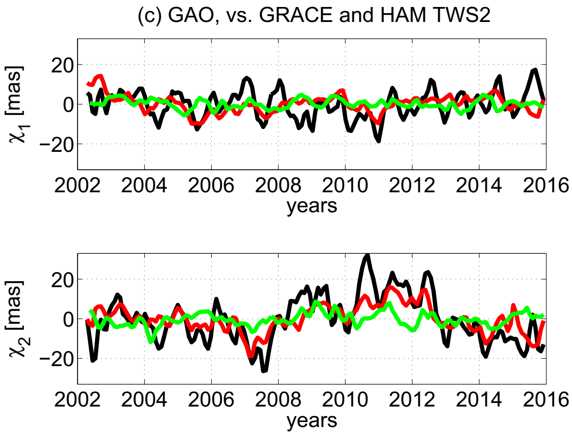

(c) GAO (black) vs. GRACE (red), TWS2 (green)

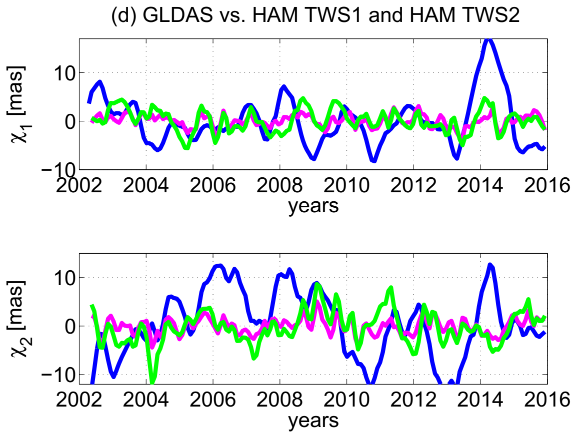

(d) TWS1 (magenta) vs. TWS2 (green), vs. GLDAS (blue)

Figure 4. Monthly multi-annual land mass-term excitations functions of polar motion derived from observed polar motion excitations χ_1 and χ_2 (black curves) by removing AAM and OAM, hydrological contributions observed by GRACE (red curves), hydrological contributions determined from land-based climate model GLDAS (blue curves), and hydrological excitation functions determined from different output of FGOALS-g2 climate model of the CMIP5 project: (a) GAO vs. GRACE and GLDAS, (b) GAO vs. GRACE and TWS1 (magenta curves), (c) GAO vs. GRACE and TWS2 (green curves); (d) comparison of different HAM excitations: TWS1, TWS2, GLDAS.

component from FGOALS-g2 climate model of CMIP5, and (d) hydrological excitation functions computed from TWS2 component from FGOALS-g2 climate model of CMIP5 shown results in the period 2002.3 - 2015.9 for oscillations below 12 months.
As shown by Fig. 5a, the geodetic residuals GAO come from the GRACE data, especially for the χ_2 component, and oscillations above 6 months. The TWS2 HAM excitations are inversely correlated with geodetic residuals GAO, both in χ_1 and χ_2 component (Fig. 5d). Generally, at those time scales, below 12 months, it is hard to say, which HAM excitations from FGOALS-g2 climate models agree the best with geodetic residuals GAO.

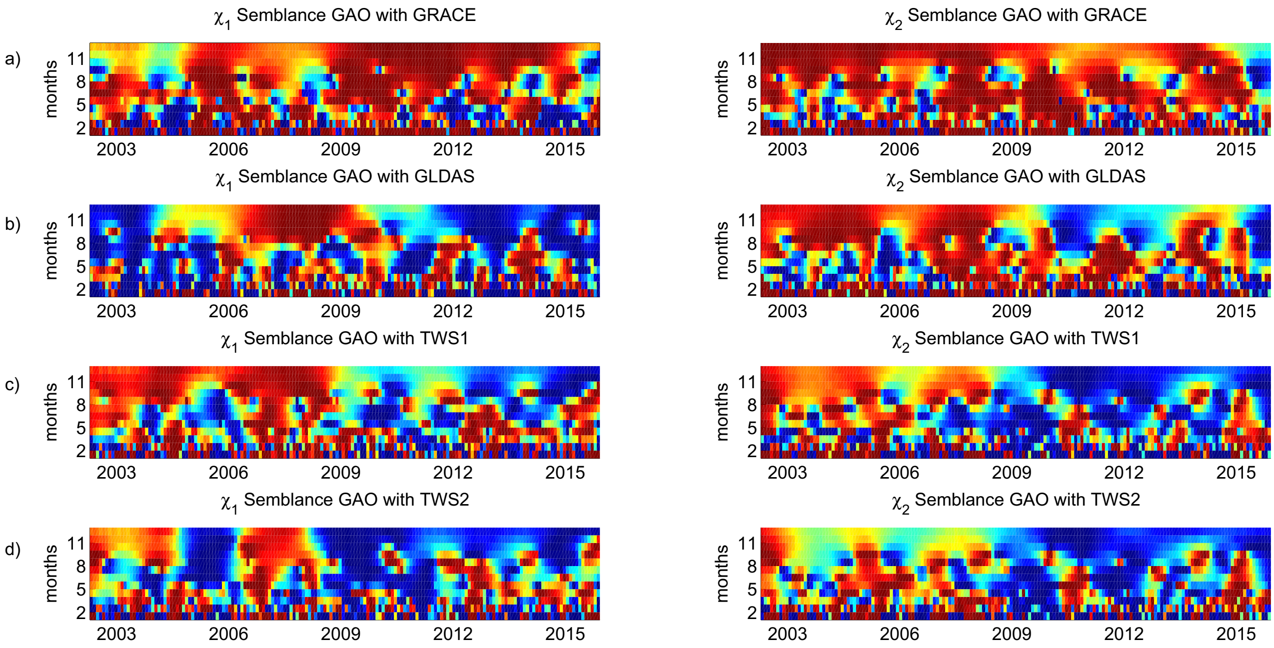

Figure 5. Semblance of dataset, χ_1 (left panel) and χ_2 (right panel) components, shown in Fig. 1 calculated withd $n = 1$. Bright red color corresponds to a semblance of $+1$, green color to a semblance of zero, and dark blue to a semblance of -1. Semblance between geodetic residuals GAO and (a) gravimetric excitation functions computed from GRACE data, (b) hydrological excitation functions computed from GLDAS climate model, (c) hydrological excitation functions computed from TWS1 component from FGOALS-g2 climate model of CMIP5, (d) hydrological excitation functions computed from TWS2 component from FGOALS-g2 climate model of CMIP5.

4. CONCLUSIONS

The hydrological excitations of polar motion determined from different variables of FGOALS-g2 climate model from CMIP5 project have been compared to geodetic residuals GAO at decadal, inter-annual and multi-annual time scales. This analysis was completed by the consideration of GLDAS global hydrological excitation functions and GRACE gravimetric excitations.
We have shown that the use of the new FGOALS-g2 climate model does not improve significantly the agreement with geodetic residuals GAO. Whereas we confirm other studies (Seoane et al., 2009, 2011; Nastula et al., 2011, 2012; Jin et al., 2010, 2012) we also indicate in details the contribution of individual variables of this climate model.

It was shown that the HAM changes obtained from FGOALS-g2 climate model do not show linear trend from 2003, expect χ_2 TWS1 HAM excitation, which the linear trend almost fits that of geodetic residuals GAO and GRACE data.
Also, TWS1 HAM excitations computed from precipitation, evaporation and runoff variables of the FGOAL-g2 climate model has the strongest prograde annual amplitudes close to prograde annual amplitudes of geodetic residuals GAO and GLDAS. The TWS1, GRACE and GLDAS HAM present almost the same retrograde annual amplitude. Semiannual oscillation of TWS1 HAM excitation is the strongest, even more powerful than the semiannual oscillation of geodetic residuals GAO.
Considering non-seasonal HAM oscillations, it is difficult to say, which hydrological excitation function from FGOALS-g2 climate model matches the best geodetic residuals GAO, GRACE data and GLDAS HAM. But the strongest amplitudes, closest to the GRACE and GAO oscillations, are noticed for the TWS2 HAM excitations computed from soil moisture and accumulated snow variables. Despite this, semblance analysis, done between geodetic residuals and TWS2 HAM, shows anti-correlation.
It is not recommended to determine hydrological excitation functions of polar motion using only soil moisture and accumulated snow water content from FGOALS-g2 climate model. Indeed, the TWS2 HAM excitations are not enough energetic to excite hydrological part of polar motion. The best agreement with geodetic residuals GAO and gravimetric excitation function of polar motion have been obtained for TWS1 HAM excitations derived from precipitation, evaporation and total surface runoff.

Acknowledgments. The research presented in this paper was supported by the Dekaban Fund program, College of Engineering, University of Michigan, Ann Arbor.

REFERENCES

Barnes R. T. H., Hide R., White A. A. and Wilson C. A. (1983). Atmospheric Angular Momentum Fluctuations, Length-of-Day Changes and Polar Motion *Proc. R. Soc. Lond. A* 1983 387 31-73; DOI: 10.1098/rspa.1983.0050. Published 9 May 1983

Bizouard C., and Gambis D. (2009). The combined solution C04 for Earth orientation parameters consistent with international terrestrial reference frame 2005 *In: H. Drewes (ed.), Geodetic Reference Frames, IAG Symposium* Munich, Germany October 9-14, 2006, Springer, Berlin 265-270.

Brzezinski A., Nastula J., Kolaczek B., and Ponte R. M. (2005). Oceanic excitation of polar motion from interseasonal to decadal periods, In *A window on the Future Geodesy* ed. F. Sanso,IAG Symposia, Vol. 128, Springer Verlag, Berlin Heidelberg, 591-596.

Brzezinski A., Nastula J., and Kolaczek B. (2005) Seasonal excitation of polar motion estimated from recent geophysical models and observations *J. Geodyn.,* 48, 235-240, doi: 10.1016/j.jog.2009.09.021.

Chao B. F., and Au A. Y. (1991). Atmospheric excitation of the Earth's annual wobble: 1980-1988, *J. Geophys. Res.,* 96, 6577-6582, doi:10.1029/91JB00041.

Chao B. F., and O'Connor W. P. (1988). Global surface water-induced seasonal variations in the Earth's rotation and gravitational field, *Geophys. J.,* 94,263-270, doi:10.1111/j.1365-246x.1988.tb05900.x.

Chen J. L., Wilson C. R., Chao B. F., Shum C. K., and Tapley B. D. (2000). Hydrologic and oceanic excitation to polar motion and length-of-day variation, *Geophys. J. Int,* 141(1), 149-156. Doi:10.1046/j.1365-246X.2000.00069.x.

Chen J. L., Wilson C. R., Tapley B. D., and Ries J. C. (2004). Low degree gravitational changes from GRACE: validation and interpretation, *Geophys. Res. Lett.,* 31(22):L22607 Doi:10.1029/2004GL021670.

Chen J. L., and Wilson C. R. (2005). Hydrological excitation of polar motion, 1993-2002, *Geophys. J. Int,* 160, 833-839, doi:10.1029/2003GL018688.

Chen J. L., Wilson C. R., Ries J. C. and Tapley B. D. (2013). Rapid ice melting drives Earth's pole to the east, *Geophys. Research Lettres,* 40, 2625–2630, doi:10.1002/grl.50552.

Cooper G. R. J., and Cowan D. R. (2008). Comparing time series using wavelet-based semblance analysis, *Computer Geosciences,* 34, 95-102, doi:10.1016/j.cageo.2007.03.009.

Dickey J. O., Marcus S. L., Johns C. M., Hide R., and Thompson S. R. (1993). The oceanic contribution to the Earth's seasonal angular momentum budget, *Geophys. Res. Lett.,* 20, 2953-2956, doi:10.1029/93GL03186.

Dobslaw H., Dill R., Groetzsch A., Brzezinski A., and Thomas M. (2010). Seasonal polar motion excitation from numerical models of atmosphere, ocean, and continental hydrosphere, *J. Geophys. Res.,* doi:10.1029/2009JB007127.

Eubanks T. M. (1993). Variations in the Orientation of the Earth, *In: D. E. Smith and D. L. Turcotte (eds.), Contributions of Space Geodesy to Geodynamics: Earth Dynamics,* American Geophysical Union, Washington, DOI: 10.1029/GD024p0001.

Gross R. S., Fukumori I. , and Menemenlis D. (2003). Atmospheric and oceanic excitation of the Earth's wobbles during 1980-2000, *J. Geophys. Res.,* 108(B8), 2370, doi:10.1029/2002JB002143.

Güntner A. (2008). Improvement of global hydrological models using GRACE data, *Surv. Geophys.,* 29(4-5):357-397.

Hinnov L. A., and Wilson C. R. (1987) An estimate of water storage to the excitation of polar motion, *Geophys. J. R. Astr. Soc.,* 88,437-459.

Van Hylckama T. E. A. (1970). Water balance and Earth unbalance, *International Associations of Scientific Hydrology,* Proc. Reading Symp. World Water Balance, AIHS-UNESCO, vol. 92, 434-444.

Jin S. G., Chambers P. , and Tapley D. (2010). Hydrological and oceanic effects on polar motion from GRACE and models, *Journal of Geophysical Research,* doi:10.1029/2009JB006635.

Jin S. G., Hassan A. , and Feng G., P. (2012). Assessment of terrestrial water contributions to polar motion from GRACE and hydrological models, *Journal of Geodynamics,* 62, 40-48, Earth Rotation, Edited by R. Gross, H. Schuh and Cheng-Li Huang, doi:10.1016/j.jog.2012.01.009.

Kolaczek B., Nuzhidina M., Nastula J., and Kosek W., (2000). El Niño impact on atmospheric polar motion excitation, *Journal of Geophysical Research B,* vol. 105, no. 2, pp. 3081-3087.

Kosek W., (1995). Time variable band pass filter spectra of real and complex-valued polar motion series, *Artif. Satell. Planet. Geod.,* 30(1), 283-299.

Kuehne J. and Wilson C. R. (1991). Terrestrial water storage and polar motion , *J. Geophys. Res.,* 96, 4337-4345.

Lettenmaier, D. P., and Famiglietti J. S. (2006). Hydrology: Water from on high, *Nature,* 444, 562-563, doi:10.1038/444562a.

Li L. J., and Coauthors, (2013). The Flexible Global Ocean-Atmosphere+Land System Model, Grid-point Version 2.0: FGOALS-g2, *Adv. Atmos. Sci.,* 30(3), 543-560, doi: 10.1007/s00376-012-2140-6.

Meyrath, T. and van Dam, T. and Weigelt, M. and Cheng, M. (2013). An assessment of degree-2 Stokes coefficients from Earth rotation data, 323 pp., *Geophysical Journal International*, 1, vol. 195, 249–259 , doi: 10.1093/gji/ggt263

Munk W. H. and MacDonald G. J. F. (1960). The rotation of the Earth, 323 pp., *Cambridge University Press*, New York.

Nastula J. and Ponte R. M. (1999). Further evidence of oceanic excitation of polar motion, *Geoph. J. Int.,* 139, 1, 123-130, doi: 10.1046/j.1365-246X.1999.00930.x.

Nastula J., Ponte R. M., and Salstein D. (2007). Comparison of polar motion excitation series derived from GRACE and from analyses of geophysical fluids, *Geophys Res. Lett.,* doi: 10.1029/2006GL028983.

Nastula J., Pasnicka M., and Kolaczek B. (2011). Comparison of the geophysical excitations of polar motion from the period: 1980.02009.0, *Acta Geophysica,* 59(3),561-577, doi: 10.2478/s11600-011-0008-2.

Nastula J., Salstein A., D. (2012). Regional Geophysical Excitation Functions of Polar Motion over Land Areas, *S. Kenyon et al. (eds.), Geodesy for Plane Earth,* International Association of Geodesy Symposia 136, doi: 10.1007/978-3-642-20338-1_59.

Nastula J., Salstein A., D., and Popinski W. (2015). Hydrological Excitations of Polar Motion from GRACE Gravity Field Solutions *International Association of Geodesy Symposia,* doi: 10.1007/1345_2015_85.

Oleson K., W., and Coauthors (2004). Technical description of the community land model (CLM), NCAR/TN-461+STR, 174 pp.

Ponte R. M., Stammer D., and Marshall J. (1998). Oceanic signals in observed motions of the Earth's pole of rotation, *Nature,* 391, 476479, doi:10.1038/35126.

Rodell M., Beaudoing K. H. (2007). GLDAS Noah Land Surface Model L4 monthly 1.0 x 1.0 degree Version 2.0,version 020, *Greenbelt, Maryland, USA:Goddard Earth Sciences Data and Information Services Center (GES DISC),* doi:10.5067/QN80TO7ZHFJZ.

Salstein D. A., Rosen R. D., Kann D. M., and Miller A. J. (1993). The Sub-bureau for Atmospheric Angular Momentum of the International Earth Rotation Service: A Meteorological Data Center with Geodetic Applications, *Bull. Amer. Meteor. Soc.,* 74, 67-80, $doi : http : //dx.doi.org/10.1175/1520 - 0477(1993)074 < 0067 : TSBFAA > 2.0.CO; 2$.

Seoane L., Nastula J. Bizouard C., and Gambis D. (2009). The use of gravimetric data from GRACE mission in the understanding of polar motion variations, *Geophys. J. Int.,* 178:614-622, doi: 10.1111/j.1365-246X.2009.04181.x.

Seoane L., Nastula J. Bizouard C., and Gambis D. (2011). Hydrological Excitation of Polar Motion Derived from GRACE Gravity Field Solutions, *International Journal of Geophysical,* 2011, Article ID 174396, 10 pages, 2011, doi:10.1155/2011/174396.

Seitz F., Schmidt M. (2005). Atmospheric and oceanic contributions to Chandler wobble excitation determined by wavelet filtering, *Journal Geophysical Res.,* 110:B11406, doi: 10.1029/2005JB003826.

Wahr J. and Molenaar M. (1998). Time variability of the Earth's gravity field: Hydrological and oceanic effect and their possible detection using GRACE, *J. Geophys. Res.,* 103, 30, 205-30,230, doi:10.1029/98JB02844.

Wahr J. (1983). The effects of the atmosphere and oceans on the Earth's wobble and on the seasonal variations in the length of day: II Results, *Geophys. J. R. Astron. Soc.,* 74, 451-487.

Received: 2016-01-12,
Reviewed: 2016-08-18 and 2016-10-07,
Accepted: 2016-10-25.